6th European Conference on Computational Mechanics (ECCM 6)
7th European Conference on Computational Fluid Dynamics (ECFD 7)
1115 June 2018, Glasgow, UK

FUNDAMENTALS OF LAX-WENDROFF TYPE APPROACH TO HYPERBOLIC PROBLEMS WITH DISCONTINUITIES

Jiequan Li[1,2]

[1]Laboratory of Computational Physics, Institute of Applied Physics and Computational Mathematics, Beijing, P. R. China
[2] Center for Applied Physics and Technology, Peking University, Beijing, P. R. China
li_jiequan@iapcm.ac.cn

Key words: Hyperbolic Problems, ccmpressible fluid flows, shocks, material interfaces, Lax-Wendroff type methods, generalized Riemann problem (GRP) method

Abstract. This lecture presents the understanding of the fundamentals when designing a numerical schemes for hyperbolic problems with discontinuities as parts of their solutions. The fundamentals includes the consistency with hyperbolic balance laws in integral form rather than PDE form, spatial-temporal coupling, thermodynamic consistency for computing compressible fluid flows, convergence arguments and multidimensionality etc. . Some numerical results are shown to display the performance

1 Introduction

This lecture presents the recent progress we made when hyperbolic problems, if their solutions contain discontinuities such as shocks and material interfaces, are computed. Due to the presence of discontinuities, the governing equations of the hyperbolic problems have to be understood in integral form (weak sense, distributional sense etc), rather than in purely differential form. Prototype examples are problems around compressible fluid flows, in which shocks are ubiquitous. Most of traditional numerical methods for such a family of problems are based on the differential form with various techniques near discontinuities. We can refer to [1, 22] and references therein for going over the development.

One of most fundamental methods representing the solution of hyperbolic problems can trace back to Cauchy-Kowalevski in 1700's [4], and the approximate solutions are represented in terms of power series using the prescribed data on non-characteristic surfaces. The numerical realization of this approach is made by Lax and Wendroff in 1960's [15], mainly for one-dimensional hyperbolic conservation laws. The resulting scheme is the celebrated Lax-Wendroff scheme and has irreplaceable values at least in the following sense.

(i) It is a unique three-point second order accurate scheme. Any high order scheme should be consistent with the Lax-Wendroff method when it reduces to the second

order version. Therefore the Lax-Wendroff method is the reference of all high order accurate methods.

(ii) It uses the least stencils (just three points for each solution value at each time step) and is most compact. Useless information is adopted as least as possible.

(iii) The Lax-Wendroff approach is a temporal-spatial coupled method and the fully useful information of the governing equations are incorporated into the scheme. Thus, there is no need to exert extra effort if any other physical or geometrical effects are included.

Nevertheless, the Lax-Wendroff approach just works for smooth flows, and it should be modified to adapt for capturing discontinuities. The currently-used generalized Riemann problem (GRP) method is regarded as the discontinuous version of L-W method, and it uses both the Cauchy-Kowalevski methodology and tracks the singularity [2, 3, 7, 5]. Moreover, the resulting scheme is consistent directly with the corresponding balance law, i.e, the weak form of the underlying governing equations, rather the partial differential equations. Hence the GRP approach avoids the large disparity from the "true" solution if strong discontinuities are present. Hence we will interpret detailed fundamentals behind the GRP approach.

This lecture will discuss the fundamentals of this family of methods, in terms of spatial-temporal coupling, thermodynamics, transversal effect and some engineering applications.

2 Lax-Wendroff method and the generalized Riemann problem method

Consider hyperbolic conservation laws,

$$u_t + f(u)_x = 0, \tag{1}$$

where $f(u)$ is the flux function. We denote by Δx the spatial increment, by Δt the time increment, $I_j = (x_{j-\frac{1}{2}}, x_{j+\frac{1}{2}})$ the computational cell interval with $x_{j+\frac{1}{2}} = (j+\frac{1}{2})\Delta x$, $x_j = j\Delta x$, $t_n = n\Delta t$. The Lax-Wendroff method in [15] uses the Taylor series expansion to design the scheme,

$$u_j^{n+1} = u_j^n - \frac{\Delta t}{\Delta x}[f_{j+\frac{1}{2}}^{LW} - f_{j-\frac{1}{2}}^{LW}], \tag{2}$$

where u_j^n can be understood as the point value of solution at (x_j, t_n), and the numerical flux $f_{j+\frac{1}{2}}^{LW}$ is taken as

$$f_{j+\frac{1}{2}}^{LW} = f_{j+\frac{1}{2}}^n + \frac{\Delta t}{2}\left(\frac{\partial f(u)}{\partial t}\right)_{j+\frac{1}{2}}^n, \qquad \frac{\partial f(u)}{\partial t} = f'(u)\frac{\partial u}{\partial t}, \qquad \frac{\partial u}{\partial t} = -f'(u)\frac{\partial u}{\partial x}. \tag{3}$$

Here $f_{j+\frac{1}{2}}^n$ is approximated upwind or using simple average from both sides, $\frac{\partial u}{\partial x}$ can be approximated using some difference quotient. This is a temporal-spatial coupling method.

with second order accuracy both in space and time. The coupling results from the substitution of spatial variation into temporal evolution.

The Lax-Wendroff scheme can be also written in the finite volume framework over the control volume $[x_{j-\frac{1}{2}}, x_{j+\frac{1}{2}}] \times (t_n, t_{n+1})$, and (2) is reinterpreted as

$$\begin{aligned} u_j^n &= \frac{1}{\Delta x}\int_{x_{j-\frac{1}{2}}}^{x_{j+\frac{1}{2}}} u(x,t_n)dx, \\ f_{j+\frac{1}{2}}^{LW} &= f(u(x_{j+\frac{1}{2}}, t_n + \frac{\Delta t}{2})) = \frac{1}{\Delta t}\int_{t_n}^{t_{n+1}} f(u(x_{j+\frac{1}{2}}, t))dt + \mathcal{O}(\Delta t^2). \end{aligned} \tag{4}$$

The issue is how to approximate $f(u(x_{j+\frac{1}{2}}, t + \frac{\Delta t}{2}))$. A direct Taylor approximation, as in [15], inevitably produces oscillations near discontinuities (if they exist), and even leads to the collapse of the corresponding simulations if the approximation has no constraint. There were a lot of achievements, particularly around limiter technology, on improving the Lax-Wendroff approach to resolve discontinuities such as the flux limiter approach [12, 13] and MUSCL type approach [25] etc. We will follow the latter framework to address the fundamentals.

Assume that given initial data for (1) at $t = t_n$ in the form

$$u(x, t_n) = P_j(x), \quad x \in (x_{j-\frac{1}{2}}, x_{j+\frac{1}{2}}), \tag{5}$$

where $P_j(x)$ is reconstructed function, with possible discontinuities at each cell interface $x = x_{j+\frac{1}{2}}$. The reconstruction technology is not repeated here and the readers are referred to e.g., [1] for details. The generalized Riemann problem (GRP) method is based on the resolution of the generalized Riemann problem for (1) subject to the initial data (5). The solution strongly depends on the associated *Riemann problem* (after suitable translation),

$$\begin{aligned} &v_t + f(v)_x = 0, \\ &u(x,0) = \begin{cases} v_- := P_j(x_{j+\frac{1}{2}} - 0), & x < 0, \\ v_+ := P_{j+1}(x_{j+\frac{1}{2}} + 0), & x > 0. \end{cases} \end{aligned} \tag{6}$$

The solution $v(x,t)$ is self-similar $v(x,t) = v(x/t, 1)$. Particularly we denote the value $u_{j+\frac{1}{2}}^n := v(0,1)$. Thanks to the regularity in time, we can take the standard Taylor expansion (only) in time to obtain

$$u(x_{j+\frac{1}{2}}, t) = u(x_{j+\frac{1}{2}}, t_n + 0) + \frac{\partial u}{\partial t}(x_{j+\frac{1}{2}}, t_n + 0)(t - t_n) + \mathcal{O}(\Delta t^2), \quad t_n < t < t_{n+1}. \tag{7}$$

It turns out that the flux can be approximated within second order accuracy

$$f_{j+\frac{1}{2}}^{GRP} = f(u_{j+\frac{1}{2}}^{n+\frac{1}{2}}), \quad u_{j+\frac{1}{2}}^{n+\frac{1}{2}} = u(x_{j+\frac{1}{2}}, t_n + 0) + \frac{\Delta t}{2}\frac{\partial u}{\partial t}(x_{j+\frac{1}{2}}, t_n + 0). \tag{8}$$

The value $u^n_{j+\frac{1}{2}} := u(x_{j+\frac{1}{2}}, t_n + 0) = u^n_{j+\frac{1}{2}}$ is given by a Riemann solver for (1)- (6). We refer to [3, 11, 23] for exact or approximate Riemann solvers. The GRP solver serves to approximate the value

$$\left(\frac{\partial u}{\partial t}\right)^n_{j+\frac{1}{2}} = \frac{\partial u}{\partial t}(x_{j+\frac{1}{2}}, t_n + 0). \tag{9}$$

Obviously, this could be achieved using the Lax-Wendroff approach, if the solution is smooth around the grid point $(x_{j+\frac{1}{2}}, t_n)$. Otherwise, we obtain the value (9) in the following

(i) *Acoustic approximation.* As $\|v_- - v_+\| \ll 1$, only linear waves emanate from $(x_{j+\frac{1}{2}}, t_n)$. Then (1) can be locally linearized as

$$u_t + f'(u_{j+\frac{1}{2}})u_x = 0, \tag{10}$$

and the value $(\partial u/\partial t)^n_{j+\frac{1}{2}}$ is computed to be

$$\left(\frac{\partial u}{\partial t}\right)^n_{j+\frac{1}{2}} = -f'(u_{j+\frac{1}{2}}) \left(\frac{\partial u}{\partial x}\right)^n_{j+\frac{1}{2}}. \tag{11}$$

The value $\left(\frac{\partial u}{\partial x}\right)^n_{j+\frac{1}{2}}$ is embodied in the initial data $P_j(x)$.

(ii) *Nonlinear GRP solver.* As $\|u_- - u_+\| \gg 1$, the genuinely nonlinear GRP solver has to be adopted. This was originally derived in [2] for gas dynamics and extended with a lots of applications [3]. This solver is derived using the nonlinear geometric optics, the tracking of singularity and the coherence of spatial and temporal variation of the flows. Later on, this method was re-accessed using the concept of Riemann invariants for general hyperbolic balance laws [7, 5, 21]. We refer to those references for details.

We conclude that the GRP flux is taken as

$$f^{GRP}_{j+\frac{1}{2}} = f(u^{n+\frac{1}{2}}_{j+\frac{1}{2}}). \tag{12}$$

This formula is always true no matter where discontinuities are present or not. The resulting scheme

$$u^{n+1}_j = u^n_j - \frac{\Delta t}{\Delta x}(f^{GRP}_{j+\frac{1}{2}} - f^{GRP}_{j-\frac{1}{2}}) \tag{13}$$

could resolve discontinuities well. In the following sections, we will state the fundamentals of the GRP scheme.

For general hyperbolic problems governed by the equations of form

$$\boldsymbol{u}_t + \nabla \cdot \boldsymbol{f}(\boldsymbol{u}) = \boldsymbol{g}(\boldsymbol{x}, \boldsymbol{u}), \tag{14}$$

we can derive the genuinely multidimensional GRP solver [17].

3 Spatial-temporal consistency with hyperbolic balance law

The GRP method provides a scheme that can be regarded as the discontinuous version of the Lax-Wendroff scheme. This method is consistent with the hyperbolic balance law

$$\frac{d\bar{u}_j(t)}{dt} = -\frac{1}{\Delta x}[f(u(x_{j+\frac{1}{2}},t)) - f(u(x_{j-\frac{1}{2}},t))], \tag{15}$$

in the sense that

$$f^{GRP}_{j+\frac{1}{2}} - \frac{1}{\Delta t}\int_{t_n}^{t_{n+1}} f(u(x_{j+\frac{1}{2}},t))dt + \mathcal{O}(\Delta t^2). \tag{16}$$

Note that this error is measured in terms of the time increment Δt, equivalently mesh size Δx, rather than the local solution variation Δu. It turns out that the GRP scheme (13) is fully consistent with the balance law (the integral form of (1))

$$\begin{aligned}\int_{x_{j-\frac{1}{2}}}^{x_{j+\frac{1}{2}}} u(x,t_{n+1})dx = & \int_{x_{j-\frac{1}{2}}}^{x_{j+\frac{1}{2}}} u(x,t_n)dx \\ & - \left[\int_{t_n}^{t_{n+1}} f(u(x_{j+\frac{1}{2}},t))dt - \int_{t_n}^{t_{n+1}} f(u(x_{j-\frac{1}{2}},t))dt\right],\end{aligned} \tag{17}$$

no matter whether the solution contains discontinuities or not. The local error is

$$E_{local} = \mathcal{O}(\Delta t^2). \tag{18}$$

Moreover, the GRP solution satisfies the "generalized" entropy inequality with tolerate error,

$$\begin{aligned}\int_{x_{j-\frac{1}{2}}}^{x_{j+\frac{1}{2}}} U(u(x,t_{n+1}))dx \le & \int_{x_{j-\frac{1}{2}}}^{x_{j+\frac{1}{2}}} U(u(x,t_n))dx \\ & - \left[\int_{t_n}^{t_{n+1}} G(u(x_{j+\frac{1}{2}},t))dt - \int_{t_n}^{t_{n+1}} G(u(x_{j-\frac{1}{2}},t))dt\right] \\ & + \mathcal{O}(\Delta t^2),\end{aligned} \tag{19}$$

where (U,F) is the entropy pair associated with (u,f) in (1). Here $u(x,t)$ is the entropy solution of (1) subject to the data (5). This shows that any possible violation of entropy inequality comes from the data reconstruction technology. Therefore, it is just this consistency that guarantees the approximate solution given by the GRP scheme (13) converges to the (weak) entropy solution of (1). All rigorous analysis can be found in [6].

4 Thermodynamic consistency

For compressible fluid flows [8], the thermodynamical (Gibbs) relation

$$Tds = de - \frac{p}{\rho^2}d\rho, \tag{20}$$

has always the fundamental importance, where T is the temperature, s is the entropy, e is the internal energy, p is the pressure and ρ is the density. Dynamically, there holds,

$$(\rho s)_t + (\rho u s)_x = 0. \tag{21}$$

Therefore, the numerical solution should implicitly satisfy

$$\begin{aligned}\int_{x_{j-\frac{1}{2}}}^{x_{j+\frac{1}{2}}} \rho s(x,t_{n+1})dx = & \int_{x_{j-\frac{1}{2}}}^{x_{j+\frac{1}{2}}} \rho s(x,t_n)dx \\ & - \left[\int_{t_n}^{t_{n+1}} \rho u s(x_{j+\frac{1}{2}},t)dt - \int_{t_n}^{t_{n+1}} \rho u s(x_{j-\frac{1}{2}},t)dt\right],\end{aligned} \tag{22}$$

with tolerate error of $\mathcal{O}(\Delta t^2)$. In the context of GRP methodology, we precisely describe entropy flux through the relation

$$\frac{\partial s}{\partial t}(x_{j+\frac{1}{2}},0+) = -u_{j+\frac{1}{2}} s'_L \frac{c_L}{c_{j+\frac{1}{2}}} \Pi(c_{j+\frac{1}{2}};0,\beta_L), \tag{23}$$

provided that a rarefaction wave moves to the left. The details can be found in [18]. The numerical result in Figure 1 shows the performance of such a thermodynamic effect.

5 Transversal effect

Most of numerical methods for hyperbolic problems construct numerical fluxes in the direction normal to each cell interface, thanks to the divergence formula, and even so for high order accurate methods if the associated Riemann solver is taken as a building block. The resulting schemes may have defects resulting from the loss of transversal effect. We have made a numeral experiment for the system linear wave equations

$$u_t + p_x = 0, \quad v_t + p_y = 0, \quad p_t + u_x + v_y = 0. \tag{24}$$

We choose the initial data as

$$p(x,y,0) = 0, \quad u(x,y,0) = v(x,y,0) = \cos(\pi(x+y)) - \cos(\pi(x-y)). \tag{25}$$

The numerical result is displayed in Table 1. The GRP method include the transversal effect using the property of spatial-temporal coupling,

$$p_t = -u_x - v_y. \tag{26}$$

The transversal variation is converted into the temporal evolution of p.

6 Multi-stage high order based on GRP solver

With the temporal consistency of the Lax-Wendroff type solver, we can design multi-stage high order schemes for hyperbolic problems. A successful example is given in [17]. Write the governing equation in the form

$$\frac{\partial \boldsymbol{u}}{\partial t} = \mathcal{L}(\boldsymbol{u}), \tag{27}$$

which is often called *the semi-discrete* form. Then the method is achieved in the following two steps.

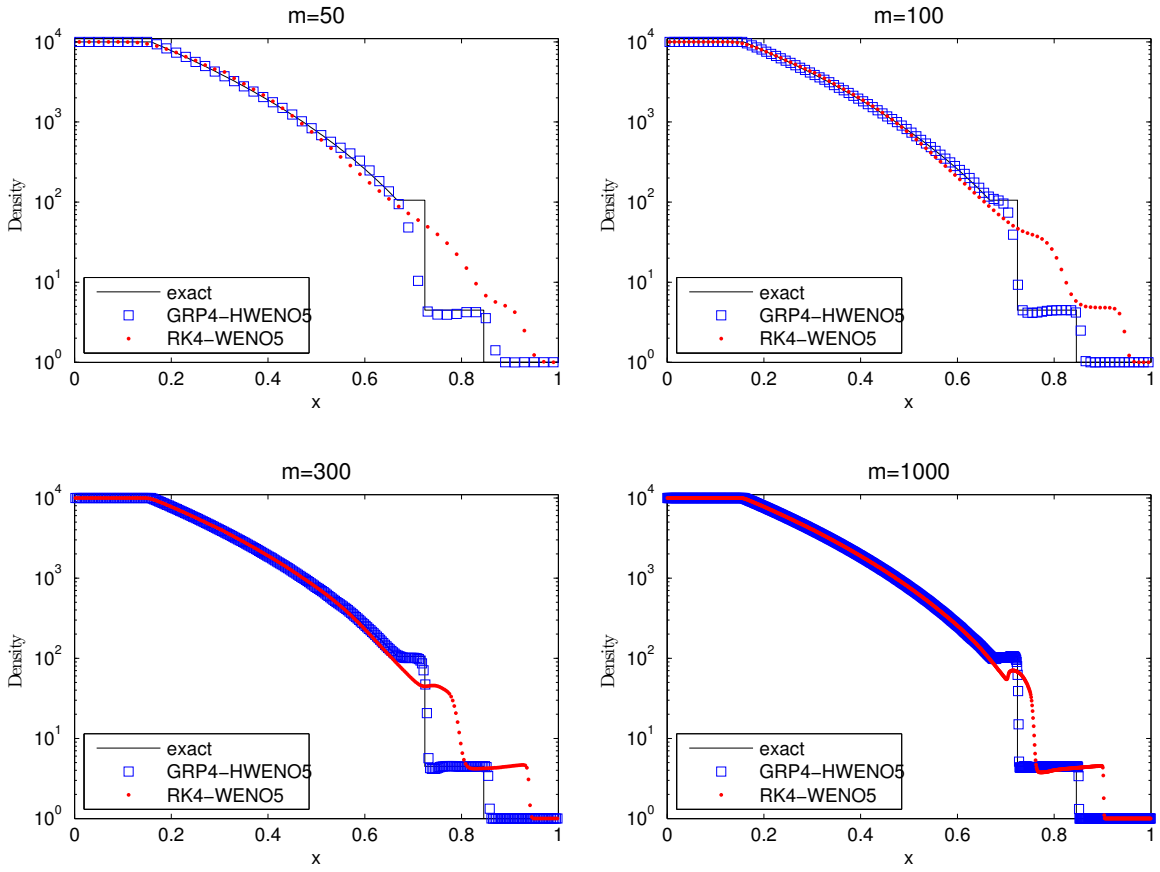

Figure 1: The comparison of the density profile for the large pressure ratio problem. The initial data is taken as $(\rho, u, p) = (10000, 0, 10000)$ for $0 \le x < 0.3$ and $(\rho, u, p) = (1, 0, 1)$ for $0.3 \le x \le 1.0$. The schemes are GRP4-HWENO5 (squares) and RK4-WENO5 (dots) with m cells.The solid lines are the exact solution.

(i) **Lax-Wendroff step**. *Given an initial data* $\boldsymbol{u}^n(x)$ *to* (1) *at* $t = t_n$, *construct instantaneous values* $\boldsymbol{u}(\boldsymbol{x}, t_n + 0)$ *and* $\frac{\partial \boldsymbol{u}}{\partial t}(\boldsymbol{x}, t_n + 0)$, *which are symbolically denoted as*

$$\boldsymbol{u}(\cdot, t_n + 0) = \mathcal{M}(\boldsymbol{u}^n), \qquad \frac{\partial}{\partial t}\boldsymbol{u}(\cdot, t_n + 0) = \mathcal{L}(\boldsymbol{u}^n). \tag{28}$$

Then $\frac{\partial}{\partial t}\mathcal{L}(\boldsymbol{u})(\cdot, t_n + 0)$ *is subsequently obtained using the chain rule,*

$$\frac{\partial}{\partial t}\mathcal{L}(\boldsymbol{u}^n) = \frac{\partial}{\partial \boldsymbol{u}}\mathcal{L}(\boldsymbol{u}^n)\frac{\partial}{\partial t}\boldsymbol{u}(\cdot, t_n + 0). \tag{29}$$

(ii) **Solution advancing step**. *Define the intermediate data* $\boldsymbol{u}^*(\boldsymbol{x})$

$$\boldsymbol{u}^* = \boldsymbol{u}^n + \frac{1}{2}\Delta t \mathcal{L}(\boldsymbol{u}^n) + \frac{1}{8}\Delta t^2 \frac{\partial}{\partial t}\mathcal{L}(\boldsymbol{u}^n), \tag{30}$$

Table 1: The L_1 error and convergence order of p for the periodic waves problem at the final time $T = 2$. The method are *GRP2D*, *RK* and *GRP1D* with $N \times N$ cells. The abbreviations mean that: GRP2D represents the genuinely 2-D GRP solver with transversal effect, RK for the two-stage Runge-Kutta method, and GRP1D for the method with the normal GRP solver.

	GRP2D		*RK*		*GRP1D*	
N	L_1 error	order	L_1 error	order	L_1 error	order
40	3.1769E-2		1.2492E-1		1.3361E-1	
80	7.9995E-3	1.99	3.0513E-2	2.03	6.3077E-2	1.08
160	2.0052E-3	2.00	7.4680E-3	2.03	3.0125E-2	1.07
320	5.0104E-4	2.00	1.8457E-3	2.02	1.9803E-2	0.61
640	1.2520E-4	2.00	4.5874E-4	2.01	1.2063E-1	−2.61

which can be used to reconstruct new initial data $\boldsymbol{u}^*(\boldsymbol{x})$ *and get the solution* $\frac{\partial}{\partial t}\mathcal{L}(\boldsymbol{u}^*)$. *Then the solution to the next time level* $t_{n+1} = t_n + \Delta t$ *can be updated by*

$$\boldsymbol{u}^{n+1} = \boldsymbol{u}^n + \Delta t \mathcal{L}(\boldsymbol{u}^n) + \frac{1}{6}\Delta t^2 \left(\frac{\partial}{\partial t}\mathcal{L}(\boldsymbol{u}^n) + 2\frac{\partial}{\partial t}\mathcal{L}(\boldsymbol{u}^*) \right). \tag{31}$$

This method can be further extended to any high order accuracy[20]. The performance is displayed in Figure 2 for capturing small scale structures.

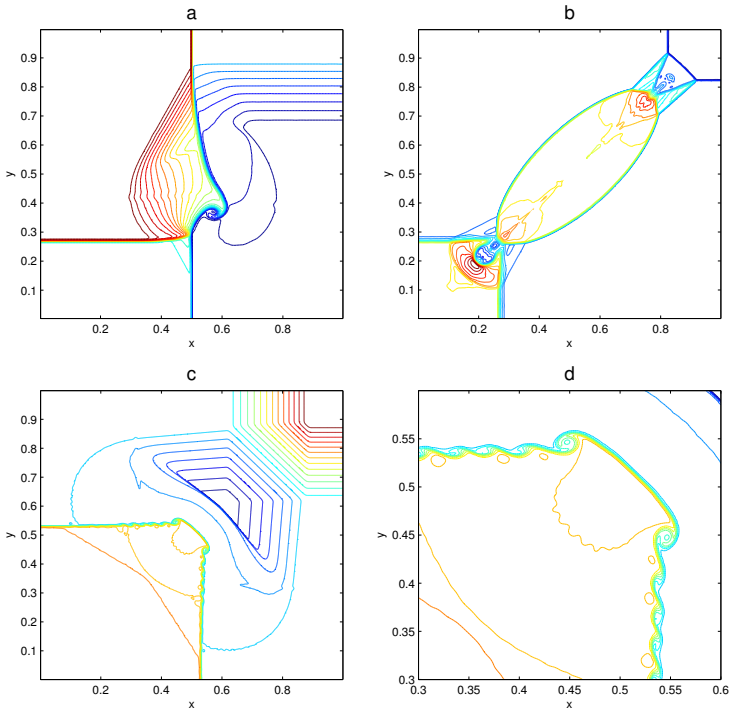

Figure 2: The density contours of three 2-D Riemann problems computed with GRP4-HWENO5. a. $[J^+_{12}S^-_{23}J^-_{34}R^+_{41}]$ with 200×200 cells. b. $[S^+_{12}J^-_{23}J^+_{34}S^-_{41}]$ with 300×300 cells. c. $[R^+_{12}J^+_{23}J^-_{34}R^-_{41}]$ with 500×500 cells. d. Local enlargement of c.

7 Discussion beyond hyperbolic problems

As far as this method is adopted for real engineering problems, the performance could be further demonstrated. For example, we simulate the following problem in [16]. Assume that a weak shock with the shock Mach number $M_s = 1.22$ propagates from atmospheric air into a stationary cylindrical bubble filled with lighter helium or heavier Refrigerant 22(R22). The computational domain $[0, 2.5] \times [0, 0.89]$ composes of 2500×890 square cells and the position of initial discontinuity is set in Figure 3. The numerical result fully agrees with the corresponding physical experiment.

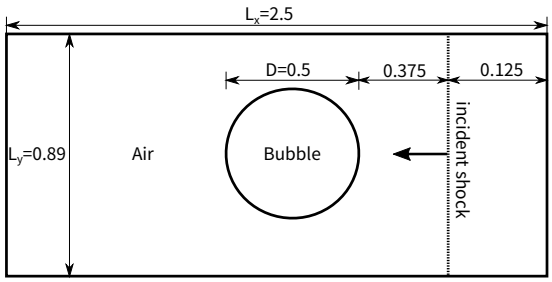

Figure 3: Diagram of the shock-bubble interaction problem

We can also extend this method the simulation of flows at the Navier-Stokes or Boltzmann level [20]. More extensions can be found e.g. in [24, 19].

Acknowlegement

Jiequan Li is supported by NSFC (No. 11771054), and foundation by LCP. I would like to thank Matania Ben-Artzi, Zhifang Du, Xin Lei, Jin Qi and Yue Wang for their contributions and a lot of discussions.

REFERENCES

[1] T. J. Barth and H. Deconinck, Herman (Eds.), High-Order Methods for Computational Physics, Lecture Notes in Computational Science and Engineering, *Springer-Verlag*, 1999.

[2] M. Ben-Artzi and J. Falcovitz, A second-order Godunov-type scheme for compressible fluid dynamics, *J. Comput. Phys.* , 55 (1984), 1–32.

[3] M. Ben-Artzi and J. Falcovitz, Generalized Riemann problems in computational fluid dynamics, *Cambridge Monographs on Applied and Computational Mathematics, 11, Cambridge University Press, Cambridge,* 2003.

[4] L. Evans, Partial Differential Equations, *Graduate Studies in Mathematics, 19, AMS*, 2002.

[5] M. Ben-Artzi and J. Q. Li, Hyperbolic conservation laws: Riemann invariants and the generalized Riemann problem, *Numerische Mathematik,* 106 (2007), 369–425.

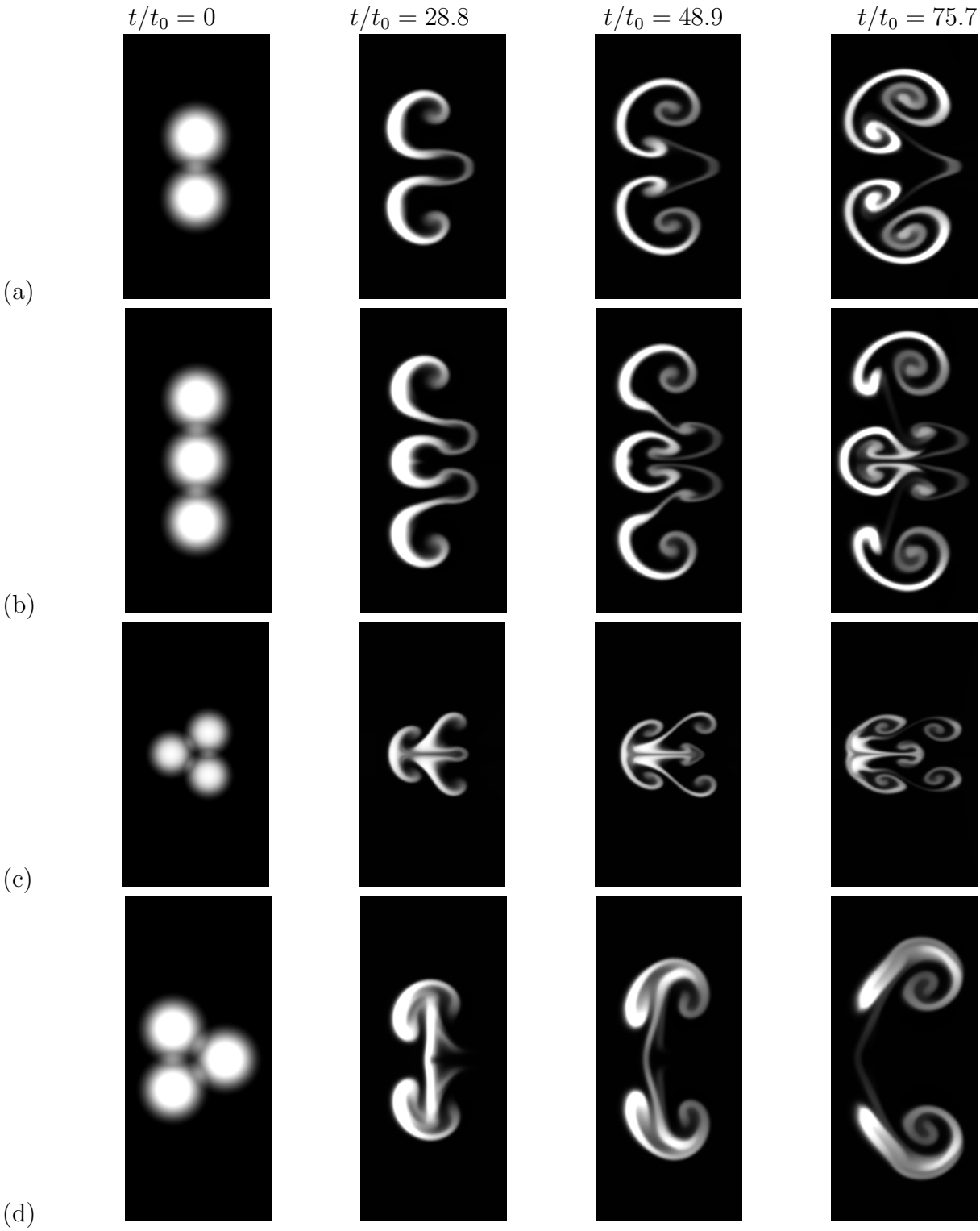

Figure 4: Gray scale images of density for the shock-accelerated SF_6 cylinders with $M_s = 1.2$ by ES-GRP with different configurations at $t/t_0 = 0, 28.8, 48.9$ and 75.7.

[6] M. Ben-Artzi and J. Li, Consistency and convergence of high order approximations to nonlinear hyperbolic conservation laws, work in preparation, 2018.

[7] M. Ben-Artzi, J. Q. Li and G. Warnecke, A direct Eulerian GRP scheme for compressible fluid flows, *J. Comp. Phys.,* 218 (2006), 19–43.

[8] R. Courant, and K. O. Friedrichs, Supersonic Flow and Shock Waves, *Springer*, 1948.

[9] B. Cockburn and C.-W. Shu, TVB Runge-Kutta local projection discontinuous Galerkin finite element method for conservation laws. II. General framework, *Math. Comp.*, 52 (1989), 411–435.

[10] Z. F. Du and J. Q. Li, A Novel Two-Stage Fourth Order Temporal Discretization Based on the Lax-Wendroff Approach, II. Viscous compressible fluid flows, *work in preparation*, 2016.

[11] S. K. Godunov, A finite difference method for the numerical computation and discontinuous solutions of the equations of fluid dynamics, *Mat. Sb.* 47 (1959), 271–295.

[12] A. Harten, High resolution schemes for hyperbolic conservation laws. *J. Comput. Phys.* 49 (1983), no. 3, 357-393.

[13] A. Harten, B. Engquist, S. Osher, and S. Chakravarthy, Uniformly high-order accurate essentially nonoscillatory schemes, III. *J. Comput. Phys.*, 71 (1987), no. 2, 231–303.

[14] G. S. Jiang, and C-W. Shu, Efficient implementation of weighted ENO schemes, *J. Comput. Phys.*, 126 (1996), 202–228.

[15] P. Lax and B. Wendroff, Systems of Conservation Laws, *Comm. Pure Appl. Math.*, Vol. XIII (1960), 217–237.

[16] X. Lei and J. Li, A non-oscillatory energy-splitting method for the computation of compressible multi-fluid flows, *Physics of Fluids,* 30 (2018), 006891.

[17] J. Li and Z. Du, A Two-Stage Fourth Order Time-Accurate Discretization for Lax–Wendroff Type Flow Solvers I. Hyperbolic Conservation Laws, *SIAM Journal on Scientific Computing*, 38 (5), A3046–A3069.

[18] J. Q. Li and Y. Wang, Thermodynamical Effects and High Resolution Methods for Compressible Fluid Flows, *J. Comput. Phys.*, 343 (2017), 340–354.

[19] J. Li, C. Zhong and C. Zhuo, A third order gas-kinetic scheme for unstructured grid *arXiv preprint arXiv:1802.00704,* 2018

[20] L. Pan, K. Xu, Q. Li and J Li, An efficient and accurate two-stage fourth-order gas-kinetic scheme for the Euler and Navier?Stokes equations, *Journal of Computational Physics*, 326 (2016), 197–221.

[21] J. Z. Qian, J. Q. Li and S. H. Wang, The generalized Riemann problems for compressible fluid flows: Towards high order, *J. Comp. Phys.*, 259 (2014) 358–389.

[22] C. -W. Shu, High order WENO and DG methods for time-dependent convection-dominated PDEs: a brief survey of several recent developments, *J. Comput. Phys.* 316 (2016), 598–613.

[23] E. F. Toro, Riemann solvers and numerical methods for fluid dynamics: A practical introducition, *Springer*, 1997.

[24] C. Wu, B. Shi, C. Shu and Z. Chen, Third-order discrete unified gas kinetic scheme for continuum and rarefied flows: Low-speed isothermal case, *Phys. Rev. E*, 97 (2018), 023306.

[25] B. van Leer, Towards the ultimate conservative difference scheme. V. A second-order sequel to Godunov's method, *J. Comp. Phys.,* 32 (1979), 101–136.